Direct manufacturing of net-shape functional components by laser consolidation process (invited paper)

Xue, Lijue

Publisher's version / Version de l'éditeur:
https://doi.org/10.3788/cjl20093612.3179
Chinese Journal of Lasers, 36, 12, pp. 3179-3191, 2009-12-01

Direct Manufacturing of Net-Shape Functional Components by Laser Consolidation Process (Invited Paper)

Lijue Xue

Industrial Materials Institute, National Research Council of Canada
800 Collip Circle, London, Ontario, N6G 4X8, Canada

ABSTRACT

Laser consolidation (LC) is a novel computer-aided manufacturing process being developed by the Industrial Materials Institute of National Research Council of Canada (NRC-IMI). This rapid manufacturing process produces net-shape functional metallic parts layer-by-layer directly from a CAD model by using a laser beam to melt the injected powder and re-solidifying it on the substrate or previous layer. As an alternative to the conventional machining process, this novel manufacturing process builds net-shape functional parts or features on an existing part by adding instead of removing material. In this review paper, laser consolidation of CPM-9V tool steel, Ni-based IN-625 and IN-718 superalloys and Ti-6Al-4V alloy will be discussed. The microstructures and functional properties of these laser consolidated materials will be examined along with several potential industrial applications.

Keywords: laser technique, materials, laser direct manufacturing, laser consolidation, net-shape, rapid manufacturing, green manufacturing

1.0 INTRODUCTION

Laser cladding based free-form fabrication is an emerging computer-aided manufacturing technology that uses a laser beam to melt injected powder (or wire) to form a solid, functional component layer by layer. This one-step computer-aided manufacturing process does not require any mould or die, and therefore provides the flexibility to quickly change the design of the components. As a result, the lead-time to produce functional parts could be reduced significantly. As opposed to the conventional machining process, this new technology builds complete parts or features on an existing component by adding rather than removing material. The parts built by the laser deposition process are metallurgically sound, free of porosity or cracks. Research work has been reported by various institutions using laser cladding based free-form fabrication technology on various alloys and steels [1-4]. Although the technology has a great potential for many industrial applications, concerns about the surface finish and dimensional accuracy have been raised.

The Industrial Materials Institute of National Research Council of Canada (NRC-IMI) has been developing laser consolidation process that takes the laser cladding based free-form fabrication technology to a new level enabling production of net-shape functional components that are difficult or even impossible to produce using conventional manufacturing technologies [5]. Research work has been published on laser consolidation of various industrials materials (such as Ni-alloys, Co-alloys, Ti-alloys, Al-alloys, stainless steels and tool steels) [5-10] and its potential for various industrial applications [11-15].

In this review paper, laser consolidation process is introduced, the microstructures and functional properties of several laser-consolidated materials are described, several case studies are presented

and the potential applications of the process for manufacturing net-shape functional components are discussed.

2.0 EXPERIMENTAL DETAILS

The laser consolidation (LC) process requires a substrate (new base or on existing component) onto which a part is built (Figure 1). A focused laser beam is irradiated on the substrate to create a molten pool, while metallic powder through a nozzle is injected simultaneously into the pool. A numerically controlled (NC) motion system (3 to 5 axes) is used to control the relative movement between the laser beam and the substrate. The laser beam and the powder feed nozzle are moved following a CAD model through a pre-designed laser path, creating a bead of molten material on the substrate, which solidifies rapidly to form the first layer. The second layer is deposited on the top of the first layer. By repeating this process, a solid thin walled structure is built. When the laser path is designed properly to guide the laser beam movement, a complex shaped part can be built directly from a CAD model without any mould or die.

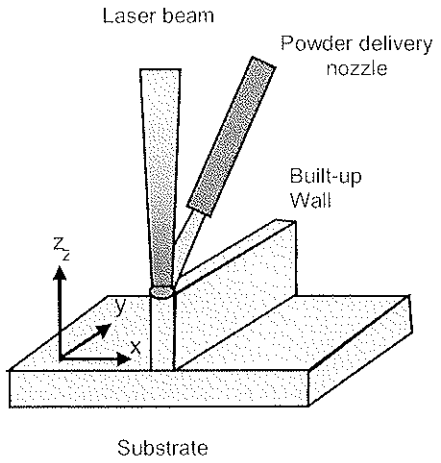

Figure 1: Illustration of laser consolidation process.

The laser consolidation work presented in this paper was conducted using a proprietary LC system developed by NRC-IMI. A 500W or 1 kW Lasag Nd:YAG laser coupled to a fiber-optic processing head was used for the experiments. The laser was operated in a pulse mode with an average power ranging from 20 to 300 W. A Sultz-Metco 9MP powder feeder was used to simultaneously deliver metallic powder into the melt pool through a nozzle with the powder feed rate ranging from 1 to 30 g/min. A 4- or 5-axis CNC motion system was used for the laser consolidation work, while processing was conducted in a glove box, in which the oxygen content was maintained below 50 ppm during the process.

Chemical compositions of the four alloy powders investigated in this paper, Ni-base IN-625 and IN-718 alloys, Ti-base Ti-6Al-4V alloy and CPM-9V tool steel, are listed in Table 1. Annealed A36 mild steel plates (0.29% C, 1.0% Mn, 0.2% Cu and Fe) with a thickness of 12.7 mm were used as the base material for laser consolidation of IN-625, IN-718 and CPM-9V materials, while wrought Ti-6Al-4V alloy substrate was used for laser consolidation of Ti-6Al-4V alloy. The substrate plates were machined and ground to a consistent surface finish for the laser consolidation of different alloy powders.

Table 1: Chemical compositions of alloy powders (wt.%)

Alloy	C	Ni	Ti	Fe	Al	Cr	Mo	Ta+Nb	V	Mg	Si
IN-625	0.03	Bal.	-	-	-	22.0	9.0	3.7	-	-	-
IN-718	0.05	Bal.	-	17.0	-	19.0	3.0	5.0	-	-	-
Ti-6Al-4V	0.07	0.02	Bal.	-	6.18	0.02	-	-	3.94	-	-
CPM-9V	1.8	-	-	Bal.	-	5.35	1.24	-	9.26	0.5	0.91

The microstructures of the LC samples were examined using an Olympus optical microscope as well as a Hitachi S-3500 scanning electron microscope (SEM). A Philips X'Pert X-ray diffraction

system was used to identify the phases of the LC materials. A 100 kN Instron Mechanical Testing System was used to evaluate the tensile properties and fatigue lives of the LC samples, while the sliding wear resistance of LC CPM-9V was evaluated using a Falex pin-on-disk tester against a 6.35 mm (1/4") diameter WC ball (HRa 92). Wear testing was conducted under a normal load of 500 g with a linear speed of 0.28 m/s running for a total sliding distance of 8000 m. The microhardness of clad materials was measured using a Buehler Micromet II Microhardness Tester.

3.0 MICROSTRUCTURES AND PROPERTIES OF SEVERAL LC MATERIALS

3.1 LC CPM-9V Tool Steel

CPM-9V is a vanadium-carbide enhanced tool steel developed by Crucible Research for powder metallurgy applications. As compared to conventional tool steels, CPM-9V exhibits excellent wear resistance [16]. CPM-9V is suitable for use in tooling which encounters severe wear, such as forming rolls, rolling mill rolls, header tooling, extrusion tooling, punches, dies, shear blades, etc.

With the optimised processing parameters, the LC CPM-9V material is fully dense, free of cracks and porosity [11]. The LC CPM-9V has a very fine microstructure, which is very hard to identify under optical microscope. A high resolution SEM photo (Figure 2a) shows that as-consolidated CPM-9V has two-phase microstructure: a light, very fine and snowflake-like phase precipitated on the dark matrix. The thickness of the light snowflake-like phase is only about 100 nm (Figure 2b). EDS analysis indicates that the light phase contains higher percentage of vanadium (about 12–14%) and chromium (about 6–6.6%) as compared to the dark matrix (about 9% V and 5.7% Cr). The XRD analysis further reveals that the light phase is $(V,Cr)_8C_7$ type carbides, while the dark one is α phase.

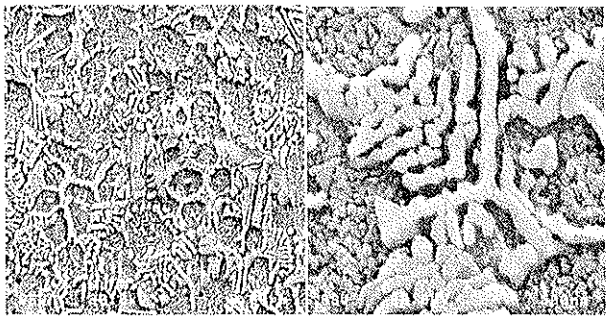

(a) (b)

Figure 2: SEM microstructure of LC CPM-9V: (a) × 6,500, and (b) × 40,000.

Table 2: Tensile properties of LC CPM-9V tool steel

Sample No.	σ_{UTS} (MPa)	$\sigma_{0.2}$ (MPa)	δ (%)	E (GPa)
#1	1358.9	883.8	2.3*	229.6
#2	1295.0	787.0	2.8*	230.6
#3	1303.8	835.9	2.2*	244.5
#4	1303.8	778.1	3.1*	232.7
Average	**1315±29**	**821±49**	**2.6***	**234±7**

LC CPM-9V material shows very good tensile properties (Table 2). Along the vertical (build-up) direction, the as-consolidated CPM-9V has average yield strength ($\sigma_{0.2}$) of 821 MPa and tensile strength (σ_{UTS}) of 1315 MPa. The elastic modulus (E) of the consolidated CPM-9V is about 234 GPa. Unfortunately, all specimens failed outside of the gauge length and therefore, the accurate

elongation data are not available. But based on the measured data within the gauge length, the average elongation (δ) of the as-consolidated CPM-9V is above 2.6%. It should be noted that all tensile test data are very consistent and the scattered ranges are small, which indicates that the laser consolidation process has good reproducibility.

LC CPM-9V also shows excellent sliding wear resistance (Figure 3). Pin-on-disk testing reveals that, under the given test conditions (tested against 6.35 mm diameter WC ball under 500 g load at a linear speed of 0.28 m/s for a total distance of 8000 m), LC CPM-9V specimens (Rc.50-55) shows significantly better wear resistance as compared to hardened D2 steel (Rc. 64-65) and normalised 4340 steel (Rc.35-36). The average volume loss of the LC CPM-9V specimens was about 0.0211 mm^3, which was only about the 1/3 of the volume loss of D2 specimens (0.0595 mm^3) and about one order of magnitude lower as compared to the 4340 specimens (0.2185 mm^3).

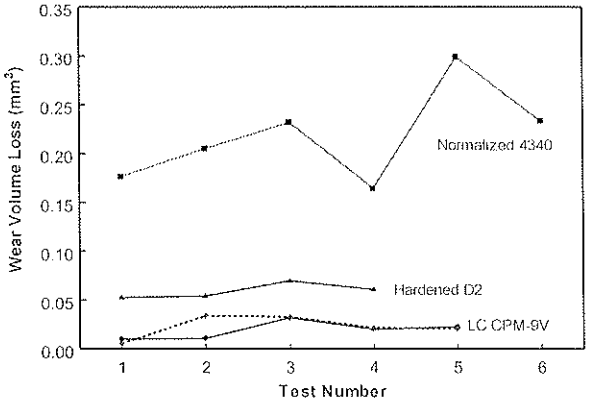

Figure 3: Pin-on-disk wear testing results (disk volume loss).

In addition, the wear loss of WC balls tested against the LC CPM-9V material was also significantly lower than that of the same balls against the D2 and 4340 steels. The average wear volume loss of the WC balls against the LC CPM-9V was only about 0.01855 mm^3, while the ball volume loss against the D2 and 4340 steels was increased double and triple (0.0417 mm^3 and 0.0538 mm^3), respectively.

It is interesting to note that although the hardness of the as-consolidated CPM-9V material is only around Rc.50-55, but its wear resistance is clearly superior to the hardened D2 steel with a hardness of around Rc. 64-65, which is consistent with the observation on powder metallurgy (P/M) CPM-9V material [16]. The excellent wear resistance of the LC CPM-9V may be attributed to the precipitation of $(V,Cr)_8C_7$ carbides due to the high vanadium contents in the alloy.

3.2 LC IN-625 Alloy

IN-625 is a solution-hardenable nickel-chromium superalloy containing molybdenum, tantalum and niobium alloying elements. It has excellent corrosion and oxidation resistance, and outstanding strength and toughness in the temperature range up to 1093°C (2000°F). The alloy has excellent fatigue strength and stress-corrosion cracking resistance to chloride ions. IN-625 alloy has been used to manufacture components for gas turbine engine ducting, combustion liners and spray bars, heat shields, furnace hardware, chemical plant hardware, and special seawater applications, etc. [17]

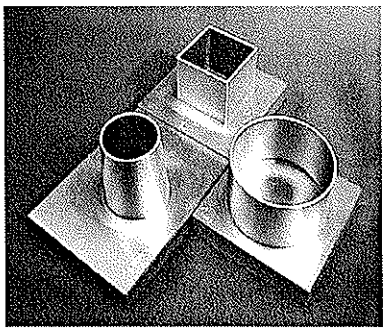

Figure 4: Three as-consolidated LC IN-625 samples.

Laser consolidation of IN-625 powder produces metallurgically sound components, free of cracks or

porosity. Figure 4 shows three LC IN-625 samples, a hollow square, a hollow cylinder and a hollow cone. These samples were prepared for measurement of the surface roughness as well as the dimensional accuracy. It is evident that LC IN-625 samples show very good surface finish. Surface roughness measurement reveals that the average roughness (Ra) of the as-consolidated IN-625 samples is about 1.5 ~ 1.8 μm [5].

The LC samples have very good dimensional accuracy. For the hollow square (25 mm × 25 mm), the standard deviation in wall thickness and height is only about 0.025 mm and 0.038 mm respectively, while the wall parallelism is within the range of 0.050 mm. The average squareness between walls is 90.00° with a deviation of 0.02°, while the average perpendicularity of square walls against the base plate is 89.92°. For the cylinder, the standard deviation in the inner and outer diameters is within 0.050 mm. For both the thin-wall cylinder and the cone, the deviation in circularity is less than 0.050 mm, while the deviation in cylindricity and conicity is 0.086 mm and 0.069 mm respectively. It is notable that the measurement of the inclined angle for the built cone is 9.93° compared to the required 10°. These errors could be attributed to the repeatability errors in the motion system as well as the errors caused by the laser consolidation process itself.

The LC IN-625 material shows unique directionally solidified microstructure due to rapid solidification inherent to the process (Figure 5). The cross-sectional view along the vertical direction (build-up direction) shows that LC IN-625 has columnar grains growing almost parallel to the build-up direction (Figure 5a), while the horizontal cross section shows that the LC IN-625 consists of fine cells of around 2-3 μm in diameter (Figure 5b). The X-ray diffraction reveals that the LC IN-625 has the same γ phase as the IN-625 powder: a face-centered cubic structure with a lattice parameter of 3.59 Å. The directional solidification of LC IN-625 material is along the (100) crystallographic plane, which is the typical dendritic growth direction of face-centered cubic structure materials [18].

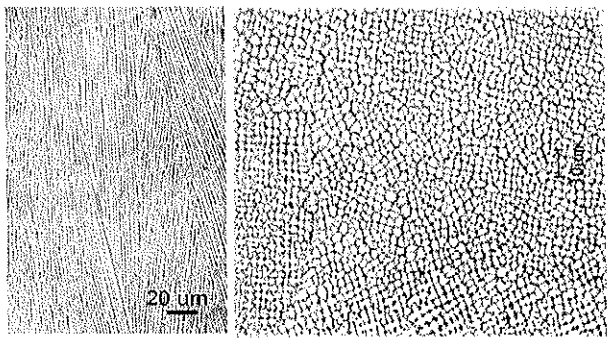

(a) (b)

Figure 5: Microstructure of LC IN-625 alloy: (a) vertical cross-sectional view, and (b) horizontal cross-sectional view.

Table 3: Tensile properties of LC IN-625 alloy

Conditions		$\sigma_{0.2}$ (MPa)	σ_{UTS} (MPa)	δ (%)
LC IN-625 (as-consolidated)	Horizontal	518±9	797±8	31±2
	Vertical	477±10	744±20	48±1
As-cast IN-625 [19]		350	710	48
Annealed wrought IN-625 [20]		490	855	50

The LC IN-625 material exhibits good mechanical properties (Table 3). Along the horizontal direction (perpendicular to the build-up direction), the yield strength and tensile strength of the LC IN-625 material are 518 MPa and 797 MPa respectively, while the elongation is about 31%. When testing along the vertical direction (parallel to the build-up direction), both the yield and the tensile strengths are slightly lower to 477 MPa and 744 MPa respectively, while the percentage elongation increases significantly to 48%. The anisotropic behaviour of the tensile

properties of the LC IN-625 alloy may be attributed to its directionally solidified microstructure. The yield strength and the tensile strength of the LC IN-625 along both directions are significantly higher than the cast IN-625 and comparable to the wrought material, although the elongation along the horizontal direction is slightly lower.

The results of the fatigue tests at room temperature are displayed in Figure 6 [21]. The LC IN-625 material tested in the build-up direction (vertical direction) had a fatigue resistance significantly higher than the investment cast but lower than the wrought material. The endurance limit of the LC material was just under 450 MPa, which is about 200 MPa higher than the investment cast material and about 100 MPa lower than the wrought material. There was essentially no difference in fatigue resistance between the 2 orthogonal directions (A and B) on wrought IN-625 sheet. In addition, the stress relieving treatment (SR) did not affect the fatigue resistance of the wrought material.

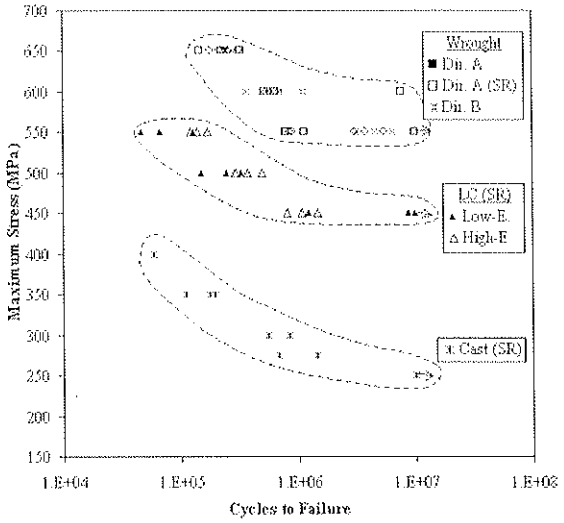

Figure 6: Fatigue testing results of IN-625 under a stress-controlled sinusoidal waveform (R = 0.1, f = 60 Hz).

In principle, the LC process is a form of casting process where the material is first melted and re-solidified in order to form a desired shape. The LC IN-625 material has essentially a cast microstructure. However, due to the rapid solidification inherent to the process, LC microstructure is much more refined and uniform as compared to the investment cast material. Furthermore, the LC material is free of cracks and porosity. This proved to be beneficial to the room temperature fatigue properties.

3.3 LC IN-718 Alloy

IN-718 is a precipitation-hardenable nickel-chromium superalloy containing significant amounts of iron, niobium, and molybdenum, along with lesser amount of aluminum and titanium. It combines good corrosion resistance and high strength with outstanding weldability, including resistance to post-weld cracking. The alloy has excellent creep-rupture strength at temperature up to 700°C (1300°F). IN-718 has been widely used as a structural material for a variety of components in gas turbines, rocket motors, spacecraft, nuclear reactors, pumps, and tooling [22].

LC processing parameters were successfully developed to build IN-718 samples with good repeatability and high integrity [10]. Similar to LC IN-625, the as-consolidated IN-718 also shows directionally solidified microstructure due to the rapid solidification inherent to the LC process (Figure 7). The cross-sectional view shows that as-consolidated IN-718 has columnar dendritic grains growing almost parallel to the build-up direction (Figure 7a), while the horizontal cross section shows fine cell structure (Figure 7b).

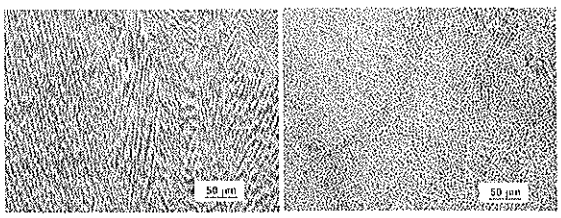

(a) (b)

Figure 7: Optical microstructure of as-consolidated IN-718: (a) vertical direction, (b) transverse direction, × 100.

The standard heat treatment procedure used for wrought IN-718 was also applied for LC IN-718 specimens: (1) solution treatment at 980°C for 1 hour followed by air cooling; (2) aging at 720°C for 8 hours followed by air cooling, and (3) aging at 620°C for 8 hours followed by air cooling. Figures 8a and 8b show optical microscopic photos of the heat-treated LC IN-718 along vertical and horizontal directions, respectively. After the heat treatment, the original columnar dendrites in LC IN-718 disappeared.

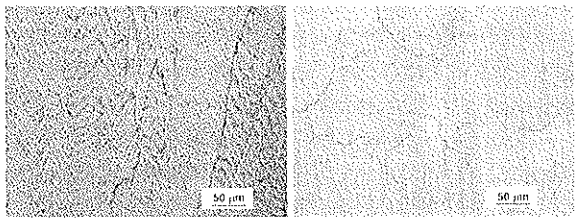

(a) (b)

Figure 8: Microstructure of heat-treated LC IN-718: (a) vertical direction, (b) transverse direction, × 200.

However, it is interesting to note that some kinds of dendritic features can still be observed under optical microscope in heat-treated LC IN-718 (Figure 8a). High resolution SEM observation reveals that those features can be attributed to carbide particles existing in the prior inter-dendritic regions and no dendritic structures remained after the heat treatment. For as-consolidated IN-718, no γ' particles can be observed. After the standard heat treatment, γ'-particles precipitated in the LC IN-718 matrix, as indicated by the significant increase in its hardness (from HV 257 increased to HV 445). However, we did not observe γ' particles under SEM with the current reagent. The work is still in progress and the results will be published later.

The X-ray diffraction (Figure 9) reveals that the as-consolidated IN-718 has the same γ phase as the IN-718 powder: a face-centered cubic structure. However, the as-consolidated IN-718 material shows a preferred orientation along the (100) crystallographic plane (the typical dendritic growth direction of face-centered cubic structure materials). It is interesting to note that, after heat treatment, the preferred orientation along (100) still remained, although its original dendrites disappeared.

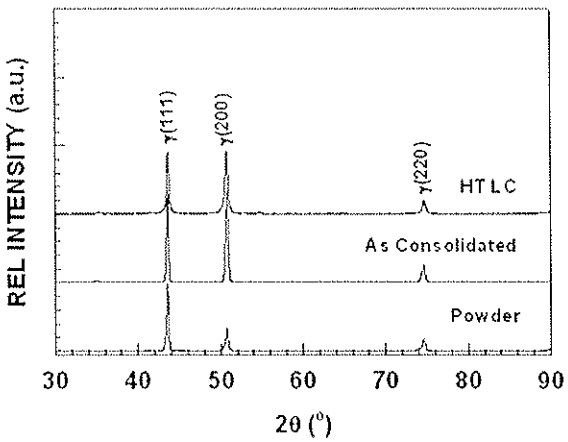

Figure 9: X-ray diffraction patterns of powder, as-consolidated and heat-treated LC IN-718.

The laser consolidation successfully produced metallurgically sound IN-718 samples, free of cracks or porosity. Due to the time limitation, we only investigated mechanical properties of LC IN-718 alloy along the vertical (build-up) direction. Table 4 compares tensile properties of LC IN-718 with various wrought IN-718 materials. The as-consolidated IN-718 alloy shows reasonably good tensile properties. The average yield and ultimate tensile strengths of the as-consolidated IN-718 are about 432 MPa and 802 MPa, respectively, while the elongation is about 39%. It should be noted that the tensile properties of the laser consolidated IN-718 material have relatively small scatter. The standard deviations of yield strength and ultimate tensile strength are only 5 MPa and 21 MPa, respectively, while the standard deviations of the elongation is about 5 %, which indicates that the laser consolidated IN-718 material has good consistency.

Table 4: Tensile properties of LC IN-718 alloy

Material	$\sigma_{0.2}$ (MPa)	σ_{UTS} (MPa)	δ (%)
LC IN-718 (as-consolidated)	432±5	802±21	39±5
LC IN-718 (HT)	1085±19	1238±12	21±2
Wrought IN-718 (HT) [22]	1036	1240	12
IN-718 Sheet (HT) [23]	1050	1280	22
IN-718 Bar (HT) [23]	1190	1430	21

After the heat treatment, the yield and tensile strengths of the LC IN-718 was increased to about 1085 MPa and 1238 MPa, respectively, while elongation was reduced to about 21 % (Table 4). The heat-treated (HT) LC IN-718 alloy demonstrates that its yield and tensile strengths, and elongation are comparable to the various types of heat-treated wrought IN-718 material. The microhardness of LC IN-718 is about HV 257 and HV 445 for as-consolidated and heat-treated conditions respectively, while the hardness of heat-treated wrought IN-718 is about HV 420 [24].

The state of residual stresses in the LC IN-718 material was measured using conventional X-ray diffraction (XRD) method. It reveals that the surface residual stress along the horizontal direction of as-consolidated IN-718 is in compression (about -297±15 MPa), while it is in tension along the vertical direction (about +121±12 MPa). After heat treatment, the residual stresses along the horizontal direction remains in compression (-245±25 MPa), while the residual stresses along vertical direction is completely eliminated (about -3±66 MPa). It should be noted that the existence of compressive residual stress in the heat-treated LC IN-718 will be beneficial to its potential application for making gas turbine engine components.

3.4 LC Ti-6Al-4V Alloy

Ti-6Al-4V is known as the "workhorse" of titanium industry, accounting for more that 50% of total titanium usage. It is an (α+β) alloy that offers a good combination of high strength, light weight, formability and corrosion resistance. Ti-6Al-4V is recommended for use at service temperature up to 350°C. It has been used for making aircraft turbine engine components, aircraft structural components, high-performance automotive parts, marine applications, medical devices, and sports equipment, etc. [25]

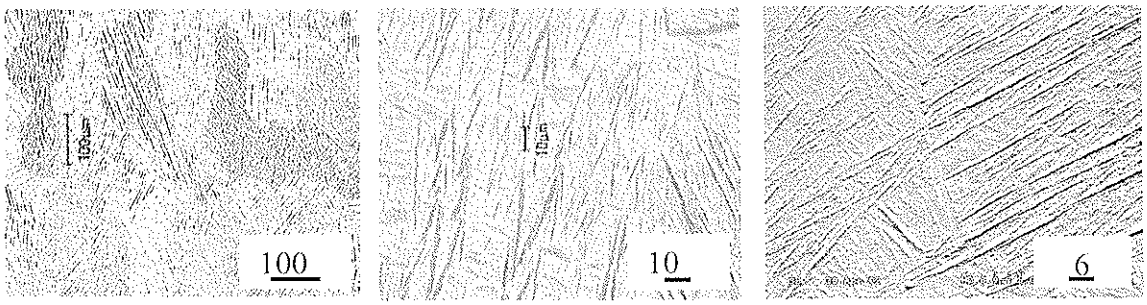

(a) Optical micrograph, ×100 (b) Optical micrograph, ×1000 (c) SEM micrograph, ×1500

Figure 10: Microstructure of LC Ti-6Al-4V.

The LC Ti-6Al-4V material is metallurgically sound. Figure 10 reveals the microstructure of the LC Ti-6Al-4V along the vertical cross-section [8]. The LC Ti-6Al-4V shows somewhat equiaxed

grains (Figure 10a) with acicular phase inside (Figure 10b). A high-resolution SEM photo reveals that grain boundary is hard to distinguish and no secondary phase can be observed along it (Figure 10c).

Ti-6Al-4V is an (α+β) alloy and its typical as-cast microstructure consists of transformed β containing acicular α as well as α at prior-β grain boundaries, while the annealed wrought Ti-6Al-4V bar typically consists of equiaxed α grain plus intergranular β [26]. X-ray diffraction (XRD) technique was used to identify the phases in the wrought, powder and LC Ti-6Al-4V. It can be seen from Figure 11 that wrought Ti-6Al-4V has majority of α phase plus small amount of β phase evidenced by the existence of β(200) peak as well as shape changes of α(101) and α(103) peaks caused by β(110) and β(211) peaks respectively. It is interesting to note that the powder Ti-6Al-4V material shows only α phase, presumably due to the rapid solidification inherent to the gas atomization process used for producing the powder.

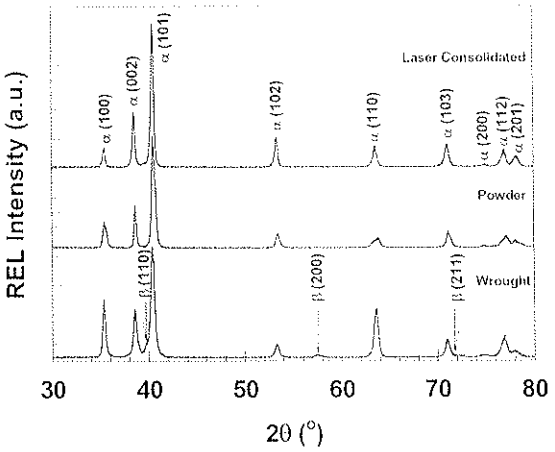

Figure 11: X-ray diffraction patterns of wrought, powder and LC Ti-6Al-4V.

The LC Ti-6Al-4V has the same phase structure as the powder used: single α-phase microstructure with α(101) as the strongest diffraction peak without any β peaks, which is consistent to the optical microscope and SEM observations. Similar to the powder Ti-6Al-4V, the lack of β phase in LC Ti-6Al-4V may also be attributed to the high cooling rate inherent to the process. Based on the optical microscope, SEM and XRD results, the LC Ti-6Al-4V microstructure consists of somewhat equiaxed α grains (transformed from β) with acicular features inside.

Table 5: Tensile properties of LC Ti-6Al-4V alloy

Materials	$\sigma_{0.2}$ (MPa)	σ_{UTS} (MPa)	E (GPa)	δ (%)
As-consolidated Ti-6Al-4V (thick-wall)	899	979	121	11.4
As-consolidated Ti-6Al-4V (thin-wall)	1062	1157	116	6.2
As-cast Ti-6Al-4V [27]	890	1035	-	10
Wrought Ti-6Al-4V (annealed) [28]	825	895	110	10
Wrought Ti-6Al-4V (solution treated and aged bar) [28]	965	1035	110	8
Wrought Ti-6Al-4V (solution heat treated + aged) [29]	1103	1172	-	10

The LC Ti-6Al-4V material exhibits very good mechanical properties. The tensile properties of the as-consolidated Ti-6Al-4V materials tested at room temperature are listed in Table 5 [30]. The yield strength and tensile strength of thin-wall (0.8 mm thick) LC Ti-6Al-4V material are 1062 MPa and 1157 MPa, respectively, while its elongation in 25 mm gauge length is 6.2%. Both tensile and yield strengths of the thin-wall LC Ti-6Al-4V are substantially higher than the as-cast/annealed cast Ti-6Al-4V and annealed wrought Ti-6Al-4V, and comparable to the heat-treated wrought Ti-6Al-4V (in solution treated plus aged condition). The elastic modulus of the

thin-wall LC Ti-6Al-4V (116 GPa) is comparable to the wrought material (110 GPa). However, the elongation of the LC material (6.2%) is lower than the cast or wrought Ti-6Al-4V (8-10%).

The thick-wall (1.5 mm thick) LC Ti-6Al-4V material was found to have a slightly lower tensile and yield strengths but a higher ductility than the thin-wall LC material. The average yield and tensile strengths of this material in the as-consolidated condition are 899 MPa and 979 MPa respectively. The average elongation is around 11.4% and the elastic modulus is slightly higher at around 121 GPa. The tensile properties of thick-wall LC Ti-6Al-4V are comparable to the as-cast (or annealed) cast Ti-6Al-4V material and better than the annealed wrought Ti-6Al-4V material.

The results of high-cycle fatigue testing are displayed in Figure 12. Both thin-wall and thick-wall LC Ti-6Al-4V specimens were tested in as-consolidated condition at room temperature. As a preliminary study, only five thick-wall LC Ti-6Al-4V specimens were tested to determine how the fatigue properties of LC Ti-6Al-4V are affected by the LC process parameters. The plot also shows reference data for cast, cast plus HIP and annealed wrought Ti-6Al-4V [31] for comparison purposes. The endurance limit shown by the thin-wall LC Ti-6Al-4V specimens is around 400 MPa, which is at the high end of the cast material scatter band. The preliminary tests conducted on thick-wall LC Ti-6Al-4V specimens have demonstrated a significant improvement in fatigue resistance over the thin-wall specimens. The results show that the endurance limit of the thick-wall LC Ti-6Al-4V material is in excess of 500 MPa, which is well within the scatter band of annealed wrought material. These preliminary results are very promising and demonstrate that the adjustment of LC processing parameters can significantly improve the fatigue properties of LC Ti-6Al-4V.

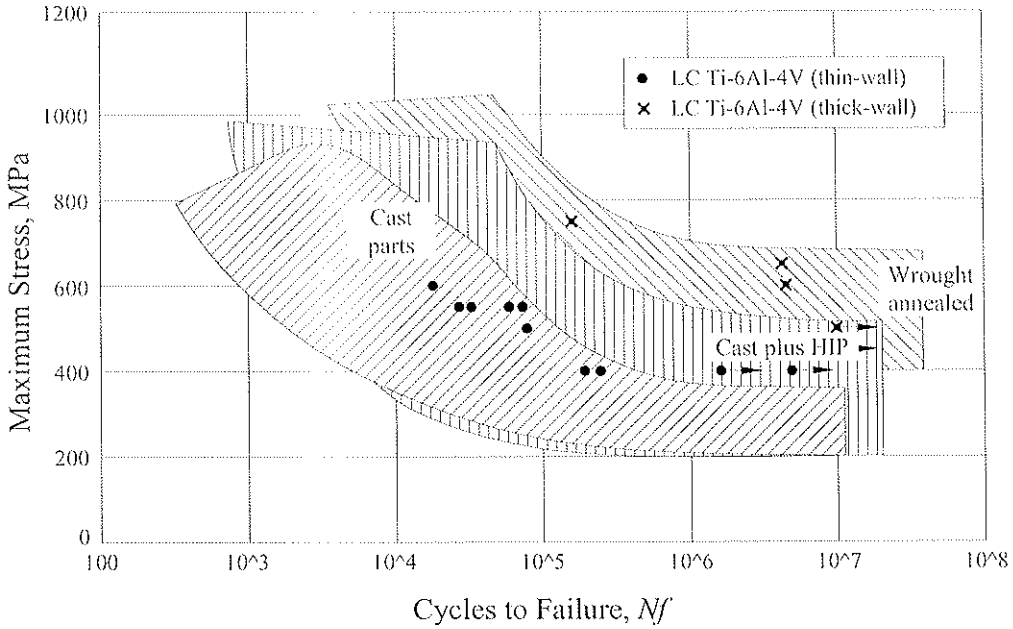

Figure 12: Fatigue data of LC Ti-6Al-4V as compared with cast and wrought/anneal Ti-6Al-4V (R = +0.1) [30].

4.0 SOME CASE STUDIES FOR INDUSTRIAL APPLICATIONS

4.1 Rotary Cutting Dies

For many applications, rotary cutting dies are very efficient and are commonly used by the industry. These high-volume, high-speed cutting dies are used for cutting a wide range of materials, such as labels, sand paper, carpet and fabric, from roll stocks, or directly in-line with printing and processing equipment, resulting in a dramatic increase in the productivity and cost savings. The manufacturing of these rotary cutting dies, however, is costly and time-consuming. Depending on the complexity of the cutting pattern and the height of the cutting blades, the entire manufacturing process may take several days or even weeks to complete. The laser consolidation process provides an exceptional capability to manufacture the rotary dies by building up cutting blades instead of machining them out from expensive tool steel stock. With this process, wear resistant materials can be used to build up the cutting blades on a low cost steel blank without the need of heat treatment. Thus, the consolidation process could significantly reduce the lead-time in the manufacturing of cutting die along with an improvement in its life. Laser consolidation of CPM-9V was investigated in collaboration with Rotoflex International for manufacturing cutting blades on low-cost steel substrate [11].

The laser consolidation process was developed to build CPM-9V cutting blades on the low alloy steel base for rotary cutting die application. With the optimised processing parameters, the LC CPM-9V blades are fully dense, free of cracks and porosity. A rectangular cutting pattern (Figure 13) was manufactured by the laser consolidation of CPM-9V material on a flat base for the dimensional accuracy measurements. The measurements were performed by using a Mitutoyo microscope equipped with an X-Y stage. Three points on each wall were selected to measure the wall thickness as well as the distance between the walls.

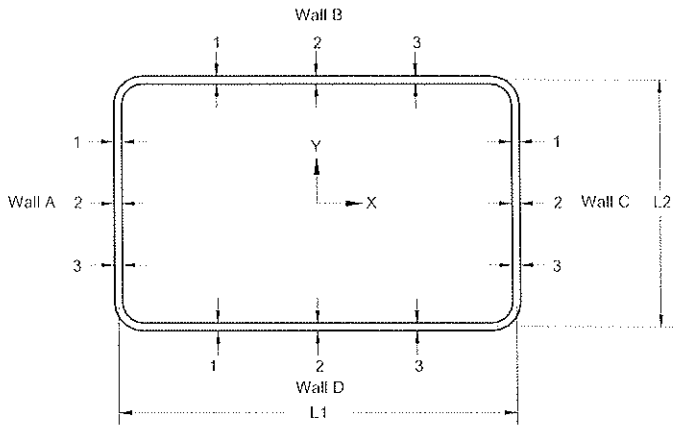

Figure 13: Details of dimensions taken for measurement on a laser consolidated rectangular cutting pattern.

Table 6: Dimensional measurement results

Dimension	Measurements (mm)			Average (mm)	Std. Deviation (mm)	Nominal (mm)	Difference (mm)
	Position 1	Position 2	Position 3				
Wall Thickness Measurement							
Wall A	0.996	1.034	1.036	1.021	0.023	-	-
Wall B	1.143	1.143	1.143	1.143	0.000	-	-
Wall C	1.001	1.008	0.927	0.978	0.046	-	-
Wall D	1.153	1.146	1.153	1.151	0.005	-	-
Wall Distance Measurement							
L1	50.744	50.764	50.800	50.770	0.028	50.800	-0.030
L2	31.463	31.463	31.471	31.466	0.005	31.496	-0.030

The measurement results (Table 6) show that the distance between walls is very uniform. The standard deviation of the three measurements for distance L1 and L2 is only about 0.028 mm and 0.005 mm respectively, and the difference between the laser consolidated wall and the CAD design is only about 0.030 mm for both cases. Wall thickness is very uniform with a standard deviation only from 0 to 0.046 mm. However, there is slightly more thickness difference between walls. The thickness of thickest Wall D is about 1.153 mm, while the thinnest wall C is only about 0.927 mm, leaving the maximum thickness difference between walls to about 0.226 mm. Because all laser-consolidated walls will be finish machined, the thickness difference will not affect the sharpening of the cutting blades as long as the distance between walls and the wall thickness are within the acceptable range.

Various types of rotary cutting dies have been successfully made by using laser consolidation process to build CPM-9V cutting blades on low cost blanks. Figure 14 shows a laser-consolidated rotary cutting die after the final sharpening. Field production testing shows that the LC CPM-9V rotary cutting dies have successfully cut more than 180,000 meters of labels without re-sharpening, while the dies made by D2 tool steel usually need re-sharpening after running the same period.

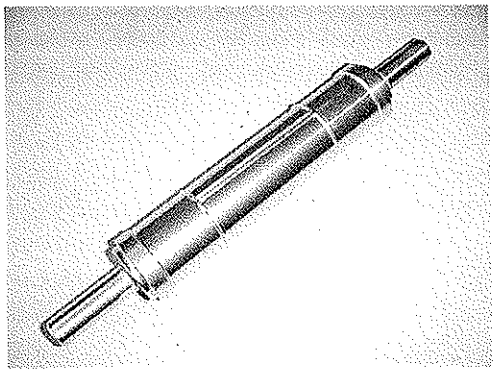

Figure 14: Laser consolidated CPM-9V rotary cutting die after final sharpening.

Based on our industrial partner's estimation, the laser consolidation process has the potential to manufacture rotary cutting dies with reduced manufacturing time by 1/3 (for dies larger than 127 mm in diameter), reduced material cost by approximately 50% and increased cutting die life by approximately 100%. In addition, with this process, worn-out cutting blades could be repaired or the same blank could be reused for building a new cutting pattern after machining out the old pattern. Die blanks can be recycled to reduce environmental impact.

4.2 Structural Components for ARMS

Advanced Robotic Mechatronics System (ARMS) project was initiated by MD Robotics and supported by the Canadian Space Agency (CSA). The main objective of this project was to investigate the use of enabling and emerging technologies for the design and manufacture of the next generation space robotic arms. In collaboration with MD Robotics and CSA, NRC-IMI utilized laser consolidation as a rapid manufacturing technology to make functional prototypes of structural components for ARMS [12].

One goal of the ARMS project was to develop a multifunctional boom structure capable of providing high structural stiffness, with dedicated features to support electronic driver/control cards and the data/power bus while allowing the dissipation of the heat generated by the electronic drivers.

Three boom shapes were initially designed: boom design #1 has an inside slot to hold an electronic board plus 4 external slots to hold wires. Boom design #2 has a slot to hold an electronic board plus an enclosed tube to hold wires inside the boom, while boom design #3 has a slot to hold an electronic board (Figure 15). All three designs provide the support for the electronic board as well as the heat dissipation. However, these multi-function, thin-walled structural components are difficult to manufacture using conventional technologies.

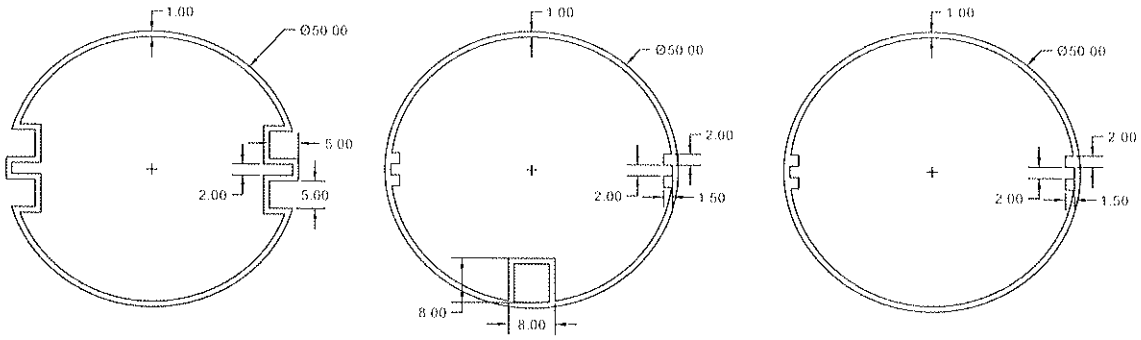

(a) Design #1 (b) Design #2 (c) Design #3

Figure 15: Initial design of boom structures.

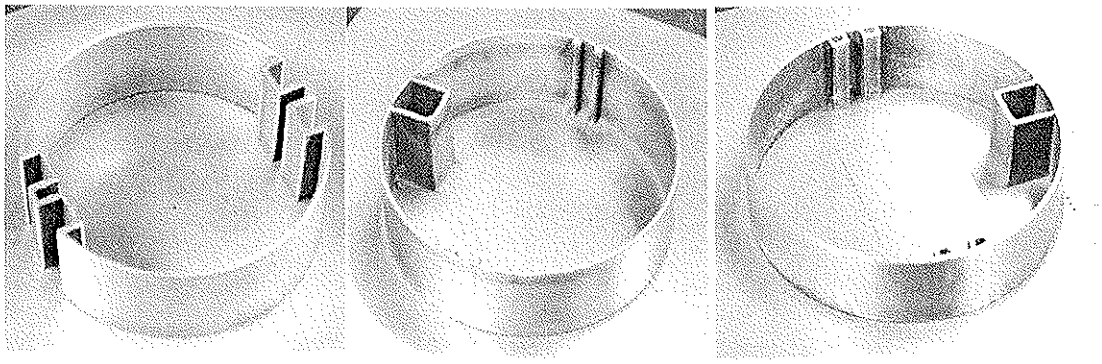

(a) (b) (c)

Figure 16: Boom structures built by LC IN-625 alloy: (a) Design #1, (b) Design #2 with slots formed by ribs, and (c) Design #2 with slots formed by rectangular tubes.

The laser consolidation process provides a unique rapid manufacturing capability to make net-shape functional prototypes to materialize these innovative designs. Figure 16a shows the boom design #1 built by using laser consolidation of IN-625 alloy. Figure 16b and 16c show the laser consolidated IN-625 boom design #2 with slots formed by ribs and rectangular tubes, respectively. It is obvious that the laser consolidation process generates high-quality functional prototypes for multi-functional boom structures that are difficult to make using conventional manufacturing technology. This study reveals that laser consolidation process can be used to accommodate specific design features, to prove design concepts and to provide versatile customization. Based on the design practice, the boom design #3 with an internal slot to hold an electronic board (Figure 15c) was finally selected as the boom design.

Figure 17: LC Ti-6Al-4V boom with a slot to hold electronic card, after final machining.

The laser consolidation process was successfully used to build the test-pieces of the multi-functional boom structure capable of providing high structural stiffness, with dedicated features to support electronic driver/control cards and the data/power bus while allowing the dissipation of the heat generated by the electronic drivers. Figure 17 shows the Ti-6Al-4V boom built using the laser consolidation process. The boom, about 270 mm in length and about 0.8 mm in

thickness, has four ribs inside to form a slot to hold electronic card. Multi-layer Ti-6Al-4V cladding was applied on both ends of the boom to enhance the local areas and four Ti-6Al-4V pads were built on the clad layer at each end to enable the connections to the housing and the payload, respectively. The LC Ti-6Al-4V boom is in as-consolidated surface finish, except the contact surfaces that were machined for final assembly.

Conventional design of a space robot manipulator generally consists of separate booms and joint housings that are connected to each other through a flanged interface, which substantially increases the weight and complexity. One-piece integrated boom/housing design is preferable to reduce the weight, complexity and increasing interface stiffness of a typical robotic arm. However, it is extremely difficult or even impossible to make the one-piece integrated boom/housing using conventional manufacturing processes. The LC process is a free-form fabrication process that allows the building of net-shape functional features on existing components. Therefore, it offers a unique capability to build multi-functional boom on pre-machined (or pre-built) housing to realize the innovative design for one-piece integrated boom/housing. Figure 18 shows an integrated boom/housing manufactured using laser consolidation of Ti-6Al-4V alloy. The integrated LC Ti-6Al-4V boom/housing shows as-consolidated surface finish, except the contact surfaces that were initially machined for next stage final machining and assembly.

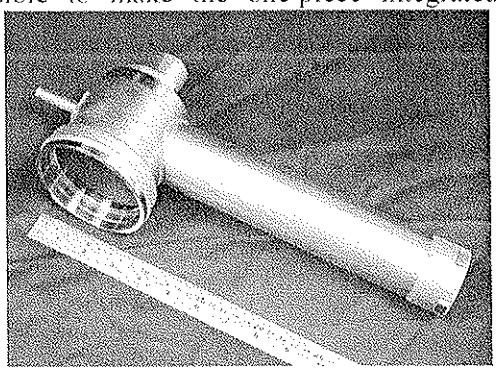

Figure 18: LC Ti-6Al-4V integrated boom/housing, after initial machining.

The Advanced Robotic Mechatronics System (ARMS) consists of four LC Ti-6Al-4V structural components:

- One Ti-6Al-4V multi-functional boom.
- Two Ti-6Al-4V housings #1 with interface.
- One Ti-6Al-4V housing #2 with integrated boom.

Laser consolidation process successfully built all above components from Ti-6Al-4V alloy. The ARMS prototype robotic joint was assembled by MD Robotics using the LC Ti-6Al-4V structural components along with the other mechanical and electronic components. Figures 19a and 19b show close views of the assembled joint and Figure 19c shows the ARMS with required payload during laboratory testing. The real time testing results demonstrated that the laser-consolidated components performed very well and all design requirements such as low weight and high strength were achieved.

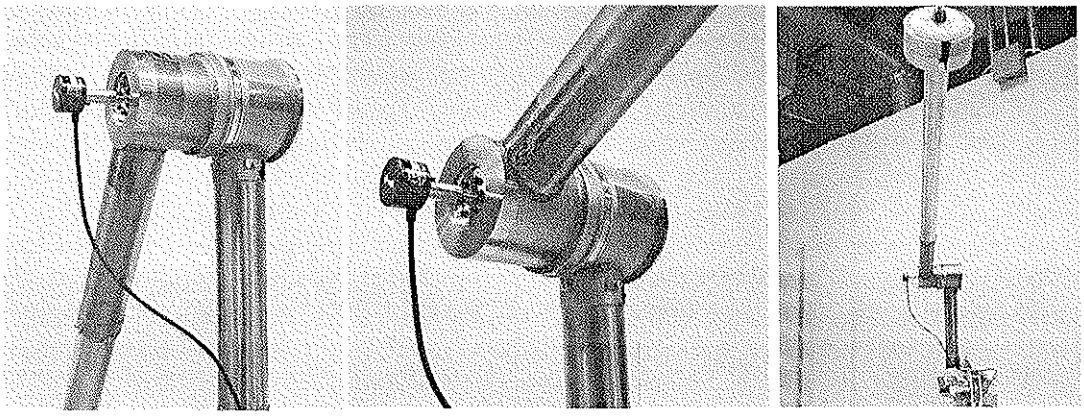

(a) (b) (c)

Figure 19: Assembled ARMS with LC Ti-6Al-4V structural components: (a) and (b) close views, and (c) testing with payload.

4.3 Shelled Structures

NRC-IMI collaborated with several companies within the scope of Precision and Freeform Fabrication Special Interest Group (PFF-SIG) to develop laser consolidation process to build functional shell structures for parts and moulds, and to investigate backfill methods to enhance the shell structures for rapid tooling applications. A unique backfill material was developed, which has good compression strength and thermal conductivity, and its thermal expansion is comparable to the laser consolidated shell. The backfilled shell structures can operate at relatively high working temperatures (above 350°C). By using the backfill method, complex cooling channels and even heating elements can be embedded into a mould (or a component) at desired locations to improve the functionality and productivity.

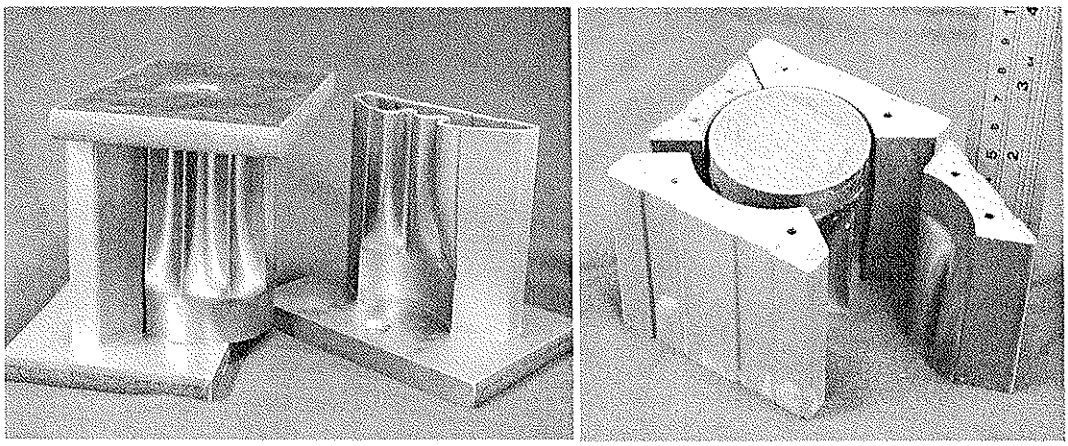

(a) (b)

Figure 20: Shell-based moulds for demonstration: (a) LC IN-625 shells, (b) 5-piece mould inserts embedded with cooling channels.

The possibility of using the laser-consolidated shell structure to make mould inserts was also demonstrated within the PFF-SIG. A mock mould with 5-piece inserts embedded with cooling channels was designed for demonstration. The mock mould consists of four external inserts and one core insert to form the cavity of a half FSP shell (max diameter of 54.6 mm and height of 64 mm). Laser consolidation process was successfully performed to build 5 pieces of the thin-wall

IN-625 alloy shell structures (Figure 20a). The laser consolidated IN-625 shells were backfilled and embedded with cooling channels to form the multi-piece mould inserts for demonstration (Figure 20b). Injection moulding testing was conducted on a simple-shaped, shell-based mould insert back-filled and embedded with cooling channels. Preliminary results reveal that the shell-based mould insert with conformal cooling demonstrated much lower subsurface temperatures and, therefore, much shorter moulding cyclic time than the solid block H13 insert baseline.

4.4 Building Features on Pre-machined Substrate or Existing Component

Laser consolidation is a material addition process that can directly build net-shape functional features on a pre-machined substrate or an existing component to form integrated structure without the need of welding or brazing, which can significantly reduce manufacturing time and material waste. Figure 21 show a demonstration piece with LC IN-625 fins built on pre-machined 316L stainless steel round bar. The LC fins have as-consolidated surface finish except their top surface that was ground. If this piece is manufactured using conventional machining, it has to start from a large round bar stock and to machine out majority of material to form the fins. Due the thin wall thickness (about 0.8 mm), it will be difficult to cast these fins and also tooling cost to make the part will be quite high for small quantity even if it can be made by casting process. Using the laser consolidation process, it readily built the required shapes, no more and no less.

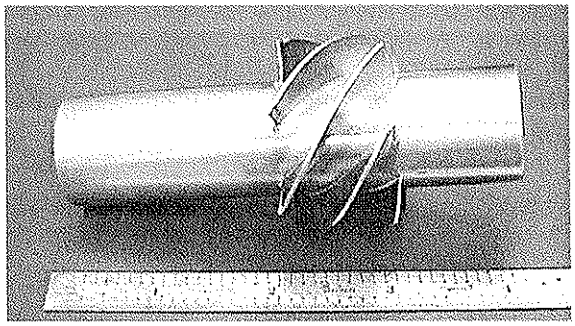

Figure 21: LC IN-625 fins built on pre-machined 316L stainless steel shaft.

Figure 22 shows two IN-718 impellers manufactured by using laser consolidation process to directly build up the blades on pre-machine substrates. It is evident that this novel process produces high quality, fairly complex shapes directly from a CAD model with good surface

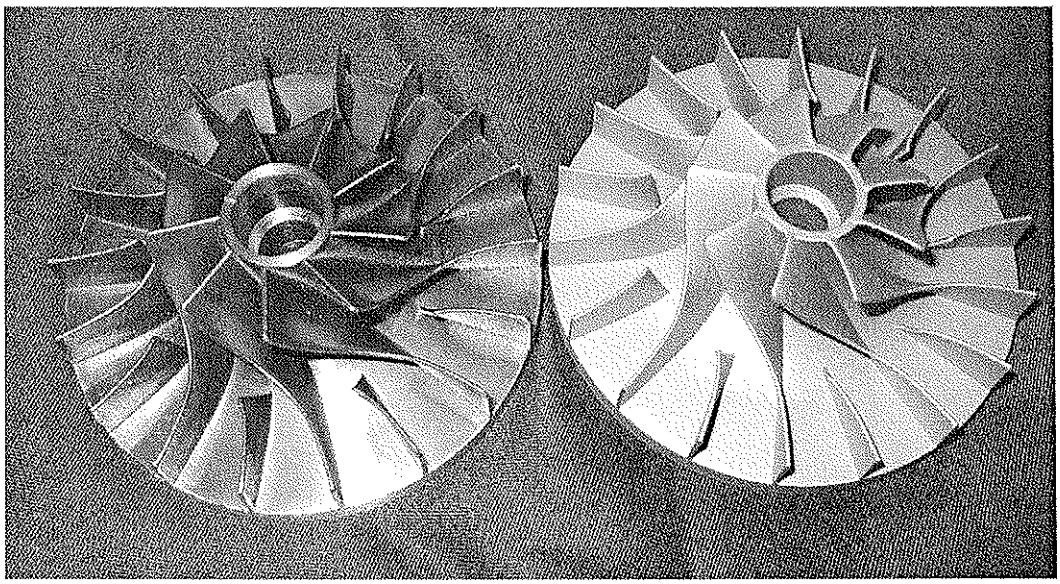

Figure 22: Demonstration impellers with LC IN-718 blades built on pre-machined substrates. Left one in as-consolidated condition; Right one after sand blasting.

finishes in as-consolidated condition without any further processing (as shown by the impeller on the left side). The bond between the LC blades and the pre-machined substrate is metallurgically sound, without crack and porosity. Compared to conventional welding process, the heat input from LC process to the substrate is minimal, resulting in a very small heat affected zone (several tens of micrometers). After sand blasting, laser consolidated blades and pre-machined substrate show consistent surface finish (as shown by the impeller on the right side) – laser consolidation process demonstrated the potential to directly manufacture net-shape functional impellers without moulds or dies. By using the LC process, more unique features can be added to the existing components to provide additional functionality, and to significantly reduce manufacturing time and cost.

5.0 CONCLUSIONS

- The laser-consolidated CPM-9V, IN-625, IN-718 and Ti-6Al-4V materials demonstrated excellent mechanical properties, which enables laser consolidation process to build functional components directly for various applications.

- Compared to other laser cladding based free-form fabrication processes that only produce near-net-shape components, the laser consolidation process provides a unique capability to build net-shape functional components or features on existing components that are difficult or even impossible to produce using conventional manufacturing processes. The laser consolidation process readily accommodates rapid design changes since no hard tooling is required.

- Laser consolidation is a green manufacturing technology that directly builds the required shapes with minimal machining. It also significantly simplifies the tooling requirements. This computer aided manufacturing process is expected to make a huge impact on manufacturing in a wide range of industries in the near future.

ACKNOWLEDGEMENT

The author would like to thank A. Theriault, Y. Li, J. Chen, S.-H. Wang, J. Jiang, G. Campbell, A. Gillett, G. Wabersich, N. Santos, B. Gibson, J. Fenner, M. Meinert for their numerous contributions in process development, sample preparation and characterization. The author would also like to take this opportunity to thank many industrial collaborators (including Rotoflex, MD Robotics, Canadian Space Agency, etc.) for their strong support in developing the technology for their specific applications.

REFERENCES

[1] Keicher, D.M., Miller, W.D., Smugeresky J.E. & Romero, J.A., Laser Engineering Net Shaping (LENS™): Beyond Rapid Prototyping to Direct Fabrication. Proceedings of the 1998 TMS Annual Meeting, San Antonio, USA, 1998, 369-377.

[2] Mazumder, J., Choi, J., Nagarathnam, K., Koch, J. & Hetzner, D., Direct Metal Deposition of H13 Tool Steel for 3-D Components. JOM, 49, 1997, 55-60.

[3] Lewis, G. K. & Schlienger, E., Practical Considerations and Capabilities for Laser Assisted Direct Metal Deposition. Materials and Design, 21, 2000, 417-423.

[4] Wu, X. and Mei, J., Near Net Manufacturing of Components Using Direct Laser Fabrication Technology. Journal of Materials Processing Technology, 135, 2003, 266-270.

[5] Xue, L. & Islam, M.U., Free-Form Laser Consolidation for Producing Metallurgically Sound and Functional Components. Journal of Laser Applications, 12(4), 2000, 160-165.

[6] Xue, L., Chen, J.-Y. & Islam, M.U., Functional Properties of Laser Consolidated Wear Resistant Stellite 6 Alloy. Powder Metallurgy Alloys and Particulate Materials for Industrial Applications, ed. by David E. Alman and Joseph W. Newkirk, 2000, 65-74.

[7] Xue, L., Chen, J.-Y., Islam, M.U., Pritchard, J., Manente, D. & Rush, S., Laser Consolidation of IN-738 Alloy for Repairing Cast IN-738 Gas Turbine Blades. Proceedings of 20th ASM Heat Treating Society Conference, St.-Louis, Missouri, USA, 2000, 1063-1071.

[8] Xue, L., Chen, J.-Y. & Theriault, A., Laser Consolidation of Ti-6Al-4V Alloy for the Manufacturing of Net-Shape Functional Components. Proceedings of 21st International Congress on Applications of Laser & Electro-Optics (ICALEO 2002), Scottsdale, Arizona, USA, 2002, 168-179.

[9] Xue, L., Chen, J.-Y. & Theriault, A., Laser Consolidation of Al 4047 Alloy. Proceedings of ICALEO 2005, Miami, Florida, USA, 2005, 344-351.

[10] Xue, L., Chen, J.-Y., Wang, S-H., Li, Y., Laser consolidation of Waspalloy and IN-718 alloys for making net-shape functional parts for gas turbine applications. Proceedings of ICALEO 2008, Temecula, California, USA, 2008, 255-263.

[11] Xue, L., Theriault, A., Chen, J., Islam, M.U., Wieczorek, A. & Draper, G., Laser Consolidation of CPM-9V Tool Steel for Manufacturing Rotary Cutting Dies. Proceedings of 10th International Symposium on Processing and Fabrication of Advanced Materials, Indianapolis, Indiana, USA, 2002, 361-376.

[12] Xue, L., Theriault, A., Rubinger, B. & Parry, D., Investigation of Laser Consolidation Process for Manufacturing Structural Components for Advanced Robotic Mechatronics System. Proceedings of the ICALEO 2003, Jacksonville, Florida, USA, 2003, 134-143.

[13] Xue, L., Theriault, A., Islam, M.U., Jones, M. & Wang, H.P., Laser Consolidation of Ti-6Al-4V Alloy to Build Functional Net-Shape Airfoils with Embedded Cooling Channels. Proceedings of the ICALEO 2004, San Francisco, California, USA, 2004, 34-40.

[14] Xue, L. & Purcell, C., Laser Consolidation of Net-Shape Shells for Flextensional Sonar Projectors. Proceedings of the ICALEO 2006, Scottsdale, Arizona, USA, 2006, 686-694.

[15] Xue, L., Li, Y., Van Daam, T. & Bampton, C., Investigation of Laser Consolidation for Manufacturing Functional Net-Shape Components for Potential Rocket Engine Applications. Proceedings of the ICALEO 2007, Orlando, Florida, USA, 2007, 161-169.

[16] Pinnow, K.E. and Stasko, W., P/M Tool Steel, Metals Handbook, 10th edition, Vol.1, ASM International, Ohio, 1990, 786-789.

[17] Inconel Alloy 625 datasheet from Special Metals website: http://www.specialmetals.com/products/inconelalloy625.php

[18] Reed-Hill, R.E., Physical Metallurgy Principles, 2nd Edition, D.Van Nostrand Company, New York, 1973, 581.

[19] Erickson, G.L., Polycrystalline Cast Superalloys. Metals Handbook, 10th Edition, Vol.1, ASM International, Ohio, 1990, 984.

[20] Morral, F.R., Wrought Superalloys. Metals Handbook, 9th Edition, Vol.3, American Society for Metals, Ohio, 1980, 219.

[21] Theriault, A., Xue, L. and Dryden, J.R., Fatigue Behaviour of Laser Consolidated IN-625 at Room and Elevated Temperatures. Materials Science and Engineering A, Vol. 516, 2009, 217-225.

[22] Mankins, W.L. and Lamb, S., Nickel and Nickel Alloys. ASM Handbook, Vol.2 Properties and Selection: Nonferrous Alloys and Special-Purpose Materials, ASM International, 1990, 438.

[23] Morral, F.R., Wrought Superalloys. Metals Handbook (9th Edition) Volume 3 Properties and Selection: Stainless Steels, Tool Materials and Special-purpose Metals, American Society for Metals, 1980, 219.

[24] Azadian, S., Aspects of Precipitation in the Alloy Inconel 718. Doctoral Thesis, Lulea University of Technology, Lulea, Sweden, 2004, 15.

[25] Titanium Alloy Ti-6Al-4V datasheet from Carpenter Technology website: http://cartech.ides.com/datasheet.aspx?i=101&E=269

[26] Boyer, R.R., Titanium and Titanium Alloys. ASM Handbook, Vol. 9: Metallography and Microstructures, ASM International, 1985, 458-475.

[27] Newman, J.R., Titanium Castings. Metals Handbook 9th Edition, Vol. 3, American Society for Metals, 1980, 409.

[28] ASM Committee on Titanium and Titanium Alloys, Properties of Titanium and Titanium Alloys. Metals Handbook 9th Edition, Vol. 3, American Society for Metals, 1980, 388-389.

[29] Davis, J.R., Titanium and Titanium Alloys. ASM Specialty Handbook: Heat-Resistant Materials, ASM International, 1997, 347-360.

[30] Theriault, A., Xue, L. and Chen, J.-Y., Laser Consolidation of Ti-6Al-4V Alloy. Proceedings of the 5th International Workshop on Advanced Manufacturing Technologies (AMT 2005), London, Ontario, Canada, 2005, 267-272.

[31] Eylon, D., Newman J.R. and Thorne J.K., Titanium and Titanium Alloy Castings.. ASM Handbook, Vol.2: Properties and Selection: Nonferrous Alloys and Special-Purpose Materials, ASM International, 1990, 642.

Dr. Lijue Xue is a Senior Research Officer with the Industrial Material Institute of National Research Council Canada and has more than 27 years experience on conducting innovative R&D on materials and manufacturing processes. He is leading the development of unique laser consolidation process to produce net-shape functional components. His research interests also include laser surface modification, joining of dissimilar lightweight materials, materials development, characterization and property evaluation.

E-mail: lijue.xue@nrc-cnrc.gc.ca